Open Access

*Catalysis Research*

LIDSEN Publishing Inc.

Editorial

# $Nb_2O_5$: Percentage Effect of T/H Phase and Evaluation of Catalytic Activity, a Preliminary Study

Michel Z. Fidelis [1, *], Elaine Trojan de Paula [2, †], Eduardo Abreu [1, †], Maria E. K. Fuziki [1, †], Onelia A. A. dos Santos [1, †], Rodrigo Brackmann [3, †], Giane G. Lenzi [2, *]

1. Departamento de Engenharia Química, Universidade Estadual de Maringá (UEM), Av. Colombo, 5790 - Bloco D90 - Zona 7, CEP 87020-680, Maringá, Brazil; E-Mails: michelmzzf@gmail.com; eduardo_abreu@live.com; mariafuziki@gmail.com; oaasantos@uem.br
2. Departamento de Engenharia Química, Universidade Tecnológica Federal do Paraná (UTFPR), Rua Doutor Washington Subtil Chueire, 330, CEP 84017-220, Ponta Grossa, Brazil; E-Mails: elainetrojandepaula@gmail.com; gianeg@utfpr.edu.br
3. Departamento de Química, Universidade Tecnológica Federal do Paraná (UTFPR), Via do Conhecimento, s/n - KM 01 - Fraron, Pato Branco - PR, 85503-390, Pato Branco, Brazil; E-Mail: rodrigobrackmann@utfpr.edu.br

† These authors contributed equally to this work.

* **Correspondences:** Michel Z. Fidelis and Giane G. Lenzi; E-Mails: michelmzzf@gmail.com; rodrigobrackmann@utfpr.edu.br

**Special Issue**: Advance in Photocatalysis

*Catalysis Research*
2023, volume 3, issue 3
doi:10.21926/cr.2303023

**Received:** September 18, 2023
**Accepted:** September 18, 2023
**Published:** September 22, 2023

**Abstract**

Due to its similar characteristics to titanium, niobium has become an attractive alternative in photocatalytic processes. Research indicates that titania has an optimal percentage of phases resulting in a commercial catalyst, P25, that contains more than 70% anatase with a minor amount of rutile and a small amount of amorphous phase. On the other hand, for $Nb_2O_5$, percentage optimization was little explored in the literature, which consists of studying the phases obtained via heat treatment individually and in different percentages via chemometric studies. In this context, the present research proposes to study the T/H phases of $Nb_2O_5$ and

their mixture. The catalysts were used to assess the catalytic activity in salicylic acid (SA) degradation. The results demonstrated that a theoretical mixture of T/H phase, with an optimal ratio of 69.1% of the H phase, had more significant SA degradation than the tests with the pure phases. The mixture was able to degrade 87.9% of SA in 60 minutes.

**Keywords**
Niobium structure; photocatalysis; salicylic acid degradation

## 1. Introduction

The so-called advanced oxidative processes (AOPs) are based on hydroxyl radicals (HO•) formation, characterized by the high oxidation capacity of several compounds to carbon dioxide, inorganic ions, and water [1]. Great emphasis is given to the study of AOPs due to the possibility of applying such methods in the recalcitrant/polluting compounds degradation into less harmful substances to the environment, as well as their use in the domestic and industrial effluents treatment.

In general, AOPs are classified into two groups: homogeneous and heterogeneous. Homogeneous systems are characterized by not using catalysts in solid form. The two most used mechanisms are direct photolysis and the generation of hydroxyl radicals using solid oxidants, such as $O_3$ and $H_2O_2$, which may or may not be combined with radiation [2, 3]. In heterogeneous systems, transition metal oxides ($TiO_2$, ZnO, $Fe_2O_3$, CdO, $SnO_2$, $Nb_2O_5$, among others) are often used, which act as photosensitizers in photocatalytic processes [4].

Currently, titanium dioxide is the most used semiconductor as a catalyst in heterogeneous system AOPs [5]. Among the characteristics that favor the $TiO_2$ used in photocatalytic reactions, the insolubility in water, high photoactivity, chemical stability in a wide pH range, and non-toxic and non-corrosive stand out [6, 7]. Titanium dioxide can be found in three crystalline forms: anatase, rutile, and brookite. They can be obtained naturally or produced artificially, but only the anatase and rutile phases are made commercially [8], under the name of P25.

P25 contains more than 70% anatase with a minor amount of rutile and a small amount of amorphous phase and is widely used due to its greater photocatalytic efficiency, but its high costs and reduced availability mean that the cost-benefit ratio is often not favorable. Because of these limiting factors for the larger scale use of $TiO_2$ P25, lines of research are increasingly interested in seeking alternative semiconductors.

The widespread use of $TiO_2$ P25 has become uneconomical for large-scale operations, such as wastewater treatment. From this perspective, $Nb_2O_5$ presents itself as a promising photocatalyst as an alternative to $TiO_2$ [9]. Using the Scopus database, it can be noticed that employing $Nb_2O_5$ as a catalyst is growing over the years, while using P25, commonly used as a reference in catalytic process, is decaying. For the niobium search, the keywords "$Nb_2O_5$" and "catalyst" were inputted, and for the P25, "P25" and "catalyst". The results can be found in Figure 1.

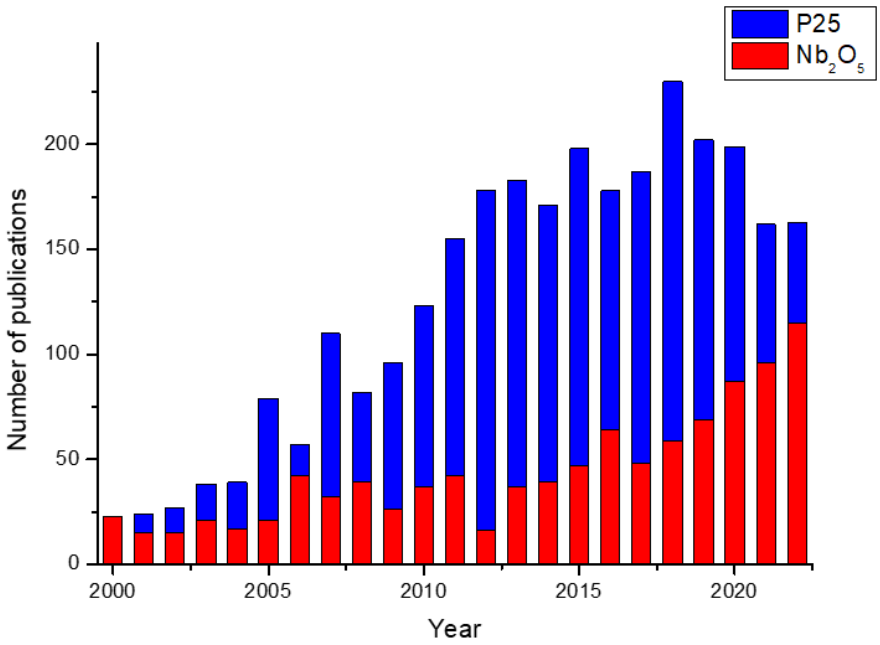


**Figure 1** Number of publications from the employing of $Nb_2O_5$ and P25 as catalysts.

In research involving heterogeneous photocatalysis, niobium oxides ($Nb_xO_y$) have been highlighted, which have properties that make them catalysts with high potential for application in this segment, especially niobium pentoxide ($Nb_2O_5$) [10]. Some similarities between $TiO_2$ and $Nb_2O_5$, such as chemical stability, non-toxicity, band gap of 3.4 eV (slightly greater than that of $TiO_2$, 3.2 eV), commercial availability and polymorphism that varies according to the processing temperature.

In this regard, Brazil holds more than 90% of the world's exploitable niobium reserves [10], standing out as the largest ore producer, with 88% of world production [11]. According to the 2022 Brazilian Mineral Yearbook, in 2021, more than 23 million tons of niobium ores (ROM) were mined in the country, with the largest niobium miners found in the cities of Araxá (MG), Catalão and Ouvidor (GO) [12]. Brazil's prominence as the largest niobium producer, combined with the similarity with $TiO_2$, further highlights the opportunity to apply this semiconductor in oxidative processes, such as photocatalysis.

Although the number of publications on using $Nb_2O_5$ as a photocatalytic semiconductor has grown over the years, little is discussed about the photocatalytic properties of each phase of this compound. There are three primary allotropic forms of $Nb_2O_5$ discovered and studied by Brauer (1941) and Schafer (1966), which occur at different temperatures (as well as $TiO_2$), namely: T phase, of structure orthorhombic (with ranges of up to 500 K), M phase, with a tetragonal structure (obtained in calcinations of up to 900 K) and H, which presents a monoclinic structure (temperatures above 1100 K). In 1955, Frevel and Rinn found a new phase of $Nb_2O_5$, obtained at temperatures lower than the T phase, called TT (pseudohexagonal structure), with a very similar structure, considered a metastable phase of the T phase with lower crystallinity [13, 14].

$Nb_2O_5$ photocatalytic activity is directly affected by its crystalline phase, as observed by Ücker et al. [15]. According to the authors, low crystallinity $Nb_2O_5$ presented degradation rates 1.2 times greater than TT- $Nb_2O_5$ phase and 5.3 times greater T-$Nb_2O_5$ phase in Rhodamine B photocatalytic removal. Kumari et al [16], in turn, noticed that monoclinic phase presented the highest photoactivity in their study on methylene blue degradation in aqueous medium. Fidelis et. al. [17]

found a found a mixture of T/TT phases with Fe/$Nb_2O_5$ catalysts calcined at 673 to 873 K, and the calcined at 873 K was the one that showed the best activity in the Triclosan and 2.8 DCDD degradation.

Thus, there is interest in studying the combination of $Nb_2O_5$ phases and its impact on the photocatalytic activity of the material. Considering that the semiconductor most used today, P25 is a synergistic mixture of the anatase and rutile phases of $TiO_2$ (which give it greater efficiency when compared to the pure phases), this work seeks to evaluate, in a preliminary study, the potential of the combination between the T and H phases of niobium pentoxide, based on its photocatalytic activity in the degradation of a model pollutant (salicylic acid, SA). A Gaussian fit was applied to the data to assess the possible synergy and optimization of the phases combination.

## 2. Materials and Methods

### *2.1 Chemicals*

Acetonitrile (HPLC-J.T. Barker, Ciudad de México, México), Methanol (HPLC- VWR chemicals, Radnor, Pensilvânia, EUA), $Nb_2O_5$, provided by the Brazilian Company of Metallurgy and Mining (CBMM), Salicylic Acid (Biotec).

### *2.2 Catalyst Heat Treatment*

All catalysts were submitted to a calcination thermal treatment to obtain the oxide precursors. Calcination is aimed at dehydrating the solid and formatting metallic oxides, exerting a great influence on the final dispersion of the active agent deposited on the support. The semiconductor was thermally treated using muffle (QUIMIS, Q318) at 873 and 1173 K, a heating rate equal to 10 K $min^{-1}$.

### *2.3 Characterization*

#### 2.3.1 X-Ray Diffractometry (XRD)

The X-ray diffractograms of the samples were obtained in a Rigaku model Miniflex 600 diffractometer with copper radiation (CuKα λ = 1.5418 Å), in the Bragg angle interval of 3° ≤ 2θ ≤ 90°, with a step of 0.05° and time fixed countdown of 2 seconds per step in semi-continuous mode. Analyzes were carried out at the Analysis Center - CA UTFPR Pato Branco.

#### 2.3.2 Physisorption of $N_2$

The nitrogen ($N_2$) physisorption method at 77 K was used for this characterization, and the equipment used was the Quantachrome Autosorb Automated Gas Sorption System. The specific area was calculated using the B.E.T method, and the pore volume and the average pore diameter were determined at a relative pressure of 0.99 by the BJH method.

#### 2.3.3 Photoacoustic Spectroscopy (PAS)

To carry out the photoacoustic spectroscopy characterization, a combination of equipment was made following the sequence of a radiation source emitting energy to a mechanical modulator that

then passes through a monochromator, filters, and reaches the photoacoustic cell, where the sample and the microphone, which emits a signal that is captured by a synchronized amplifier and which subsequently provides the intensity and phase of the photoacoustic signal, and this data is then transferred to a computer. The spectra obtained were then normalized to the carbon signal, and the direct band gap energy (Egap) of each material was obtained using the linear method (a linear fit is made in the graph of the square of the absorption coefficient versus the photon energy).

### *2.4 Analytical Control*

2.4.1 High Performance Liquid Chromatography

Analytical determination of salicylic acid (SA) concentration was carried out using a high-performance liquid chromatograph (YL Clarity 9100) equipped with a pre-column, C-18 column (Phenomenex) and visible ultraviolet (UV-VIS) detector, the wavelength at 210 nm. Elution was performed with a 40:60 Acetonitrile: Phosphate buffer (pH = 2.8, 50 mM) mixture at 1 mL $min^{-1}$ flow, following methodology adapted from Bond, 1987 [18].

### *2.5 Photocatalytic Tests*

Preliminary studies of percentage variation of $Nb_2O_5$ T/H phases with constant catalyst concentration (1 g $L^{-1}$) and solution pH (3, 5) were carried out in order to verify whether a combination of phases demonstrates greater efficiency in the photocatalytic process. The tests were carried out with the pure phases, T and H, and also with the mixtures of them in the T/H proportions equal to 0.25/0.75, 0.50/0.50 (in triplicate), and 0.75/0.25 (T/H ratio in mass). To perform this assessment, a Gaussian curve was fitted to the data found, allowing the prediction of the T/H phases ratio with the best removal efficiency. The Gaussian process has shown promise in the fields of materials science and computational kinetics, with an increase in studies being developed applying this technique [19-21].

SA degradation studies were carried out using a bench-top jacketed batch reactor, as shown in Figure 2.

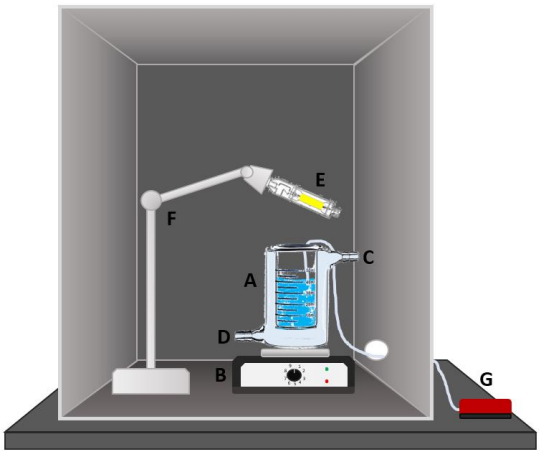


**Figure 2** Batch reactor where "A" represents the batch reactor, "B" the base for magnetic stirring, "C" the cooling liquid outlet, "D" the cooling liquid inlet, "E" the lamp for UV radiation, " F" the lamp holder and "G" the air pump [22].

Batch tests included a 600 mL capacity reactor with magnetic agitation (Tecnal, TE-424), water bath refrigeration at 20°C (Solab, model SL-152/10), oxygen air pump (12 $cm^3$ $min^{-1}$), and a 250 W mercury vapor lamp, which had its original protective bulb removed to avoid interference.

Salicylic acid was chosen as a model pollutant for the present study as it is an excellent alternative to the use of dyes, which, despite being widely used, can provide misleading interpretations of results due to issues such as spectral interference and catalyst dye-sensitization process [23]. In addition, studies indicate that the use of salicylic acid in heterogeneous photocatalysis tests can be useful in the study of reaction pathways, especially if combined with phenol, allowing the differentiation between hydroxyl radical-induced and direct charge-transfer processes [24] or TiIV-•OHsurf and TiIV-O•--TiIV pathways [18]. The SA solution was prepared in ultrapure water, with an initial concentration equal to 20 mg $L^{-1}$. The samples were removed in predetermined times, filtered into syringe filters (13 mm, pore size 0.22 µm), and injected into high-resolution liquid chromatographer (HPLC). The degradation was calculated from the peak areas presented in the chromatograms.

## 3. Results

### *3.1 Caracterizantion*

The catalysts' XRD analysis is presented in Figure 3. The peaks obtained were compared with the standards published by ICDD (International Center for Diffraction Data). Two chromatograms, one in blue and the other in red, represent different phases of $Nb_2O_5$. The blue chromatogram shows the monoclinic phase of $Nb_2O_5$, with the prominent peaks marked with the symbol "+". On the other hand, the red chromatogram represents the orthorhombic phase of $Nb_2O_5$, with the key peaks marked with the symbol "#".

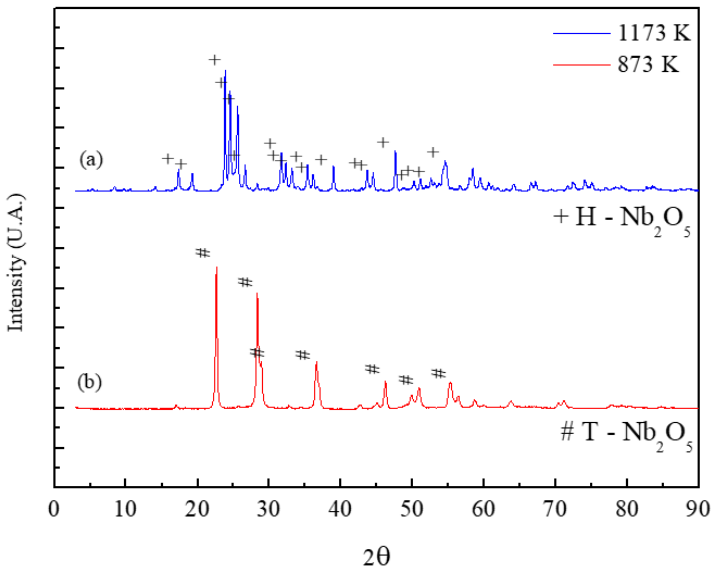


**Figure 3** X-ray diffractograms obtained for (a) $Nb_2O_5$ calcined at 1173 K and (b) $Nb_2O_5$ calcined at 873 K.

The band gap results are indicated in the Figure 4.

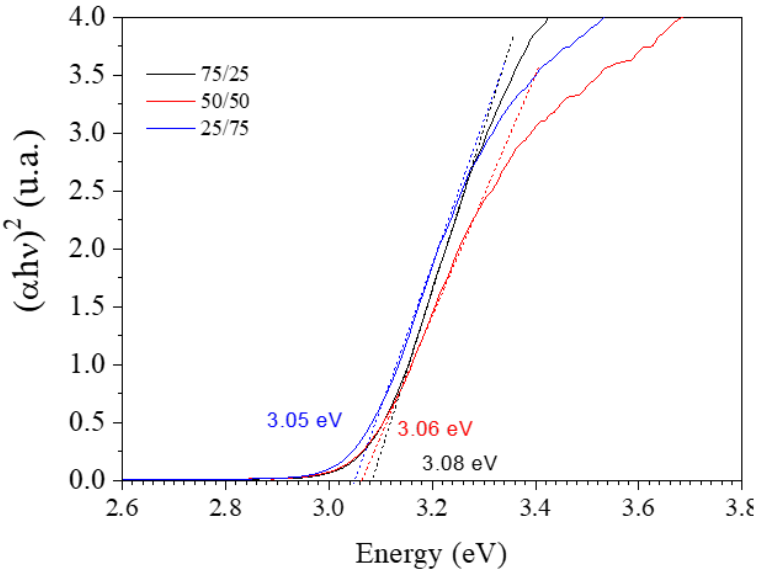


**Figure 4** Photoacoustic Spectroscopy Results.

The results of Specific surface area (S0), Pore Voluem (Vp) and Pore diameter (Dp) are presented in Table 1.

**Table 1** Textural properties of the catalysts.

| Sample (T/H phase) | $S_0$ ($m^2g^{-1}$) | Vp ($cm^3g^{-1}$) | Dp (Å) |
|---|---|---|---|
| 75/25 | 63 | 0.4307 | 272 |
| 50/50 | 67 | 0.2448 | 145 |
| 25/75 | 22 | 0.1418 | 257 |

### *3.2 Photocatalytic Tests*

Figure 5 kinetic degradation curves for different catalysts, with varying percentages of T and H phases. The degradation occurs at different rates, with the catalyst consisting of 25% T phase and 75% H phase showing the fastest degradation and the catalyst consisting of 75% T phase and 25% H phase showing the slowest degradation. At the 30-minute mark, there is a 15% difference in the degradation percentage between these two catalysts.

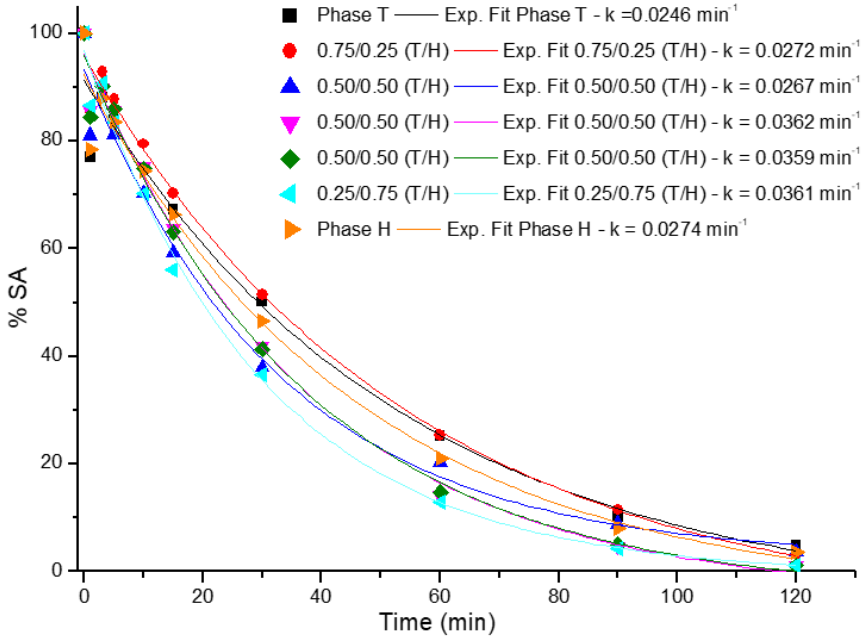


**Figure 5** Photocatalytic tests and respectively kinetic constants.

Figure 6 Gaussian curve is plotted in red based on collected data. The graph also displays each analysis carried out in triplicate in the form of a point, with its respective error bar.

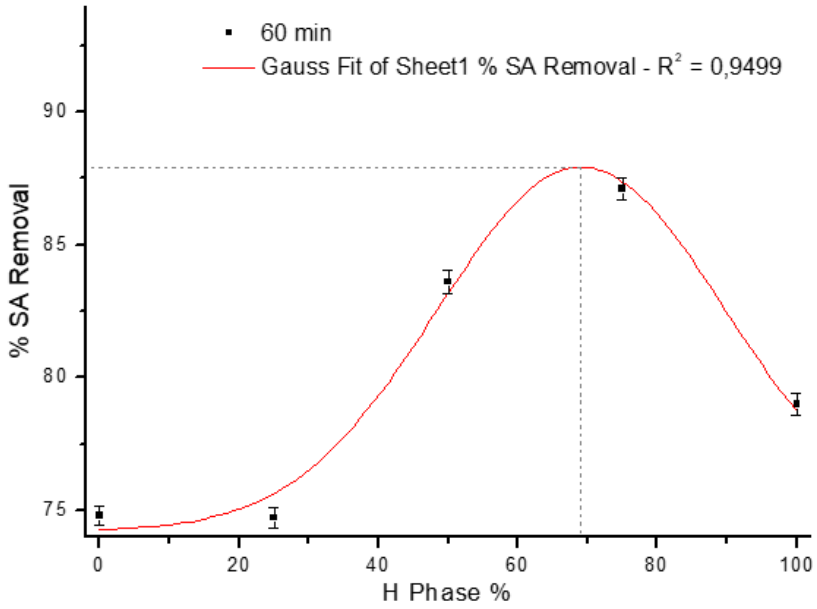


**Figure 6** Gauss Fit using the removal data at 60 min of radiation exposure.

## 4. Discussion

By analyzing the diffractograms, it is possible to verify that the catalyst it is possible to confirm that the motivation calcined at 873 K has an orthorhombic structure (T-$Nb_2O_5$) and the one calcined at 1173 K has a monoclinic system (H-$Nb_2O_5$), with the diffractograms similar to those obtained by [25] and [26]. The data obtained on the textural properties of the catalysts indicated that the T phase of 75 and 50% maintains the triggers with a specific surface area in the range of 60 $m^2g^{-1}$. On

the other hand, when we have a more significant amount of H phase, there is a decrease in the surface area. It was also observed that the volume of pores is greater the greater the amount of niobium in phase T. This influence of the phase on the specific surface area is also indicated in the literature for other materials [27]. The band gap results were in a range of 3.05 and 3.08 eV. A smaller band gap would be related to a lower energy for the electron to go from the valence band to the conduction band. The catalyst with 25% in the T phase and 75% in the H phase would be the most suitable for photocatalyzed reactions.

The photocatalytic test results can be observed in Figure 5. The final removal ranged from 95.0 to 98.8% of the initial concentration of the pollutant. The greater removal occurs in the 0.50/0.50 and 0.25/0.75 (T/H) tests, pointing that a mix of the phases are better to remove the salicylic acid than the pure phases tests. The test using the pure T phase as a catalyst, was able to remove 95% at 120 min exposure to radiation, followed by the pure H phase, which removed 96.3% at the final time. The use of mix phases showed greater removal values, such 98.8% in both the 0.50/0.50 and 0.25/0.75 (T/H) tests, which agrees with the characterization data (band gap).

For the Gaussian fit, the data at 60 min was chosen due to the advanced time, removal achieved, and the distinction between the catalysts, being able to perform a better assessment from the collected data. The Gauss fit is presented in Figure 6.

The data were able to fit the model with a good result. As noted in the tests, a mix of the phases performed better. Using the obtained model equation, the $x_c$ (center value from x, in this case, the percentage from H phase in the catalyst), is 69.1%, achieving a theorical SA removal of 87.9% at 60 min of radiation exposure. Using this model, a prediction from the behavior can be obtained, and therefore, in this way, a relation can be achieved between the phases of the catalyst and the removal of the pollutant. Statistica 7.0 software was used to calculate the experimental error in this analysis, taking into account the following arguments: Actual mean value (μ), sample mean (X), and experimental error according to Equation (1). The experimental error was calculated from the triplicate sample standard deviation. Considering 95% confidence in the data, it can be said that the experiments carried out throughout the work are within the experimental error.

$$\mu = X \pm \text{experimental error} \quad (1)$$

## 5. Conclusions

The tests carried out with the variation in the % of T/H phases of $Nb_2O_5$ in the degradation of salicylic acid allowed us to conclude that a mixture of phases, 30.9% T and 69.1% H, presented, from a model, with 95% of confidence, better photocatalytic performance. It was also possible to observe a trend towards a higher percentage of the H phase and that the pure phases presented inferior versions to the mixtures.

## Acknowledgments

The authors are thankful to the Brazilian agencies CNPq, CAPES, and Fundação Araucária for financial support of this work, C2MMa and the Central de Análises - CA for the analysis performed, and Brazilian Mining and Metallurgy Company - CBMM due to the donation of the $Nb_2O_5$.

## Author Contributions

Michel Z. Fidelis, Elaine Trojan de Paula: Investigation, Methodology, Writing - original draft, Visualization, Data curation, Eduardo Abreu, Maria E. K. Fuziki and Rodrigo Brackmann: Methodology, Writing - review & editing, Onelia A. A. dos Santos: Data curation, Writing - review & editing. Giane G. Lenzi: Conceptualization, Supervision, Writing - review & editing, Funding acquisition.

## Competing Interests

The authors have declared that no competing interests exist.

## References

1. Haynes WM. CRC Handbook of Chemistry and Physics, 95th ed. Boca Raton, FL, US: CRC Press; 2014.
2. Machulek A, Oliveira SC, Osugi ME, Ferreira VS, Quina FH, Dantas RF, et al. Application of different advanced oxidation processes for the degradation of organic pollutants. In: Organic Pollutants - Monitoring, Risk and Treatment. London, UK: InTech; 2013. pp. 141-166. Doi: 10.5772/53188.
3. Basturk E, Karatas M. Decolorization of antraquinone dye reactive blue 181 solution by UV/$H_2O_2$ process. J Photochem Photobiol A. 2015; 299: 67-72.
4. Castro DC, Cavalcante RP, Jorge J, Martines MA, Oliveira L, Casagrande GA, et al. Synthesis and characterization of mesoporous $Nb_2O_5$ and its application for photocatalytic degradation of the herbicide methylviologen. J Braz Chem Soc. 2016; 27: 303-313.
5. Silva WL, Lansarin MA, Moro CC. Síntese, caracterização e atividade fotocatalítica de catalisadores nanoestruturados de $TiO_2$ dopados com metais. Quim. Nova. 2013; 36: 382-386.
6. Fontana KB, Chaves ES, Kosera VS, Lenzi GG. Barium removal by photocatalytic process: An alternative for water treatment. J Water Process Eng. 2018; 22: 163-171.
7. Fioreze M, dos Santos EP, Schmachtenberg N. Processos oxidativos avançados: Fundamentos e aplicação ambiental. Rev Eletrônica Gest Educ Tecnol Ambient. 2014; 18: 79-91.
8. Saleiro GT, Cardoso SL, Toledo R, Holanda JN. Avaliação das fases cristalinas de dióxido de titânio suportado em cerâmica vermelha. Ceramica. 2010; 56: 162-167.
9. Souza RP, Ambrosio E, Souza MT, Freitas TK, Ferrari Lima AM, Garcia JC. Solar photocatalytic degradation of textile effluent with $TiO_2$, ZnO, and $Nb_2O_5$ catalysts: Assessment of photocatalytic activity and mineralization. Environ Sci Pollut Res. 2017; 24: 12691-12699.
10. Lopes OF. Synthesis and characterization of $Nb_2O_5$ nanoparticles and study of their photocatalytic properties. São Carlos: Universidade Federal de São Carlos; 2013.
11. United States Geological Survey. Mineral commodity summaries 2022. Liston, VA, US: United States Geological Survey; 2022. pp. 202.
12. Companhia Brasileira de Metalurgia e Mineiração. Relatório de sustentabilidade. Araxá, State of Minas Gerais, Brazil: Companhia Brasileira de Metalurgia e Mineiração; 2018. pp.104.
13. Nowak I, Ziolek M. Niobium compounds: Preparation, characterization, and application in heterogeneous catalysis. Chem Rev. 1999; 99: 3603-3624.

14. Lopes OF, Mendonça VR, Silva FB, Paris EC, Ribeiro C. Niobium oxides: An overview of the synthesis of $Nb_2O_5$ and its application in heterogeneous photocatalysis. Quim Nova. 2015; 38: 106-117.
15. Ücker CL, Riemke FC, de Andrade Neto NF, de AG Santiago A, Siebeneichler TJ, Carreño NL, et al. Influence of $Nb_2O_5$ crystal structure on photocatalytic efficiency. Chem Phys Lett. 2021; 764: 138271.
16. Kumari N, Gaurav K, Samdarshi SK, Bhattacharyya AS, Paul S, Rajbongshi B, et al. Dependence of photoactivity of niobium pentoxide ($Nb_2O_5$) on crystalline phase and electrokinetic potential of the hydrocolloid. Sol Energy Mater Sol Cells. 2020; 208: 110408.
17. Fidelis MZ, Abreu E, Dos Santos OA, Chaves ES, Brackmann R, Dias DT, et al. Experimental design and optimization of triclosan and 2.8-diclorodibenzeno-p-dioxina degradation by the Fe/$Nb_2O_5$/UV system. Catalysts. 2019; 9: 343.
18. Vione D, Picatonotto TA, Carlotti ME. Photodegradation of phenol and salicylic acid by coated rutile-based pigments: A new approach for the assessment of sunscreen treatment efficiency. J Cosmet Sci. 2003; 54: 513-524.
19. Zhang Y, Xu X. Machine learning band gaps of doped-$TiO_2$ photocatalysts from structural and morphological parameters. ACS Omega. 2020; 5: 15344-15352.
20. Ng KH, Gan YS, Cheng CK, Liu KH, Liong ST. Integration of machine learning-based prediction for enhanced model's generalization: Application in photocatalytic polishing of palm oil mill effluent (POME). Environ Pollut. 2020; 267: 115500.
21. Chow V, Phan RC, Le Ngo AC, Krishnasamy G, Chai SP. Data-driven photocatalytic degradation activity prediction with gaussian process. Process Saf Environ Prot. 2022; 161: 848-859.
22. Lenzi GG, Abreu E, Fuziki ME, Fidelis MZ, Brackmann R, de Tuesta JL, et al. 17 α-ethinylestradiol degradation in continuous process by photocatalysis using Ag/$Nb_2O_5$ immobilized in biopolymer as catalyst. Top Catal. 2022; 65: 1225-1234.
23. Barbero N, Vione D. Why dyes should not be used to test the photocatalytic activity of semiconductor oxides. Environ Sci Technol. 2016; 50: 2130-2131.
24. Bertinetti S, Minella M, Barsotti F, Maurino V, Minero C, Özensoy E, et al. A methodology to discriminate between hydroxyl radical-induced processes and direct charge-transfer reactions in heterogeneous photocatalysis. J Adv Oxid Technol. 2016; 19: 236-245.
25. Graça MP, Meireles A, Nico C, Valente MA. $Nb_2O_5$ nanosize powders prepared by sol-gel-structure, morphology and dielectric properties. J Alloys Compd. 2013; 553: 177-182.
26. Falk G, Borlaf M, Bendo T, Novaes de Oliveira AP, Rodrigues Neto JB, Moreno R. Colloidal sol-gel synthesis and photocatalytic activity of nanoparticulate $Nb_2O_5$ sols. J Am Ceram Soc. 2016; 99: 1968-1973.
27. Anschutz AJ, Penn RL. Reduction of crystalline iron (III) oxyhydroxides using hydroquinone: Influence of phase and particle size. Geochem Trans. 2005; 6: 60.